Clinical Ophthalmology

Dovepress
open access to scientific and medical research

Open Access Full Text Article

ORIGINAL RESEARCH

Meibomian Gland Probing Stimulates a Proliferative Epithelial Response Resulting in Duct Regeneration

Steven L Maskin*, Claire Toland*

Dry Eye and Cornea Treatment Center, Tampa, FL, USA

*These authors contributed equally to this work

Correspondence: Steven L Maskin, Dry Eye and Cornea Treatment Center, 3001 West Swann Ave, Tampa, FL, 33609, USA, Tel +1 813 875 0000, Email drmaskin@gmail.com

Purpose: To demonstrate that the meibomian gland ductal basement membrane and basal epithelial cell layer are in continuity with and may derive from lid margin orifice-associated rete ridge epithelial/basement membrane structures (OARREBS) and to characterize changes in the distal duct microanatomy after meibomian gland probing (MGP) using in vivo confocal microscopy (IVCM).

Patients and Methods: Pre/post-MGP IVCM examinations were performed on upper lids. Thirty-six identical glands from 20 lids of 16 patients (49.24 ±17.11 y/o with 13:3 F:M) were identified, analyzed, and compared to control cases. Statistical analyses were performed using ImageJ software and IBM SPSS version 27. All MGPs were performed within 12 weeks of the initial examination. Post-MGP follow-up exams occurred at 5.03 ±4.48 months.

Results: Post-MGP images showed more superficially organized OARREBS with accelerated and more superficial basement membrane formation, and an average increase of 32.2%, 25.4%, 32.04%, 77.7%, and 81.3% in duct wall epithelial cell layers (DWECL) ($p < 0.001$, compared to control (CTC) $p < 0.001$), distal duct wall thickness (DWT) ($p < 0.001$, CTC $p < 0.001$), proximal DWT ($p < 0.001$, CTC $p < 0.001$), distal lumen area ($p < 0.001$, CTC $p = 0.037$), and proximal lumen area ($p < 0.001$, CTC $p = 0.007$), respectively. The increase in the distal DWT and lumen area correlated with the months of follow-up ($p = 0.004$ and $p = 0.010$, respectively). Immediate post-MGP imaging revealed the probe track confined to the ductal epithelial compartment.

Conclusion: MGP appears to stimulate a proliferative epithelial response characterized by an accelerated more superficial formation of ductal basement membrane with increased DWECL as well as DWT and lumen area at two separate duct foci. These findings suggest activation of lid margin meibomian gland precursor cells and confirm that MGP stimulates an epithelial regenerative phenomenon, not a fibrotic one.

Keywords: meibomian gland probing, rete ridges, dry eye, meibomian gland dysfunction, precursor cells, meibomian gland regeneration

Introduction

Meibomian glands (MG) are modified holocrine sebaceous glands located in the eyelid tarsal plate and secrete meibum, which emerges from their orifices at the lid margin to be delivered into the tear film with blinking.[1] Obstructive meibomian gland dysfunction (MGD) is the leading type of dry eye disease whereby compromised meibomian gland function leads to a destabilized tear film resulting in increased evaporation of aqueous tears.[2] MGD has traditionally been a frustrating disease to manage. Overcoming this frustration with improved clinical outcomes may be facilitated by a greater understanding of Meibomian gland precursor cells. While the embryology of the meibomian gland has been described,[3] knowledge of the identity and location of precursor cells that support and maintain post-natal meibomian gland homeostasis remains limited in part due to difficulty delineating between precursor and early differentiated cells. Studies have suggested various locations of these precursor cells, such as the acinar periphery,[4] the acinar-ductule

Received: 30 November 2023
Accepted: 16 February 2024
Published: 1 March 2024

junction,[5] and along the central duct.[6] Though details of meibomian gland precursor cells remains unclear, *central duct integrity* appears to be necessary for acinar-ductule growth[7] suggesting an important role for intraductal gland probing in maintaining gland health by establishing or confirming the integrity and patency of the gland outflow tract free from fixed (such as periductal fibrosis) and non-fixed obstructions.[8]

A recent study proposed a new genetic cell marker of meibomian gland development and post-natal homeostasis in a mouse model, with the identification of an epithelial stem cell population. The KROX20 gene and Krox20-lineage cells were shown to be necessary to generate the full, mature meibomian gland extending from the lid margin through the entire length of the meibomian gland structure.[9] This observation is consistent with our previous ARVO 2022 study, which we report in detail within this manuscript, suggesting a cell population at the lid margin consisting of orifice-associated rete ridge epithelial/basement membrane structures (OARREBS) in continuity with and may differentiate into ductal basal epithelium and basement membrane.[10] Furthermore, these rete ridge structures may be activated by the mechanical stimulation of gland probing leading to increased duct wall epithelial cell layers and thickness (in previous studies of meibomian glands using IVCM, rete ridge structures consisting of an epithelial/basement membrane ring surrounding a dermal core (papilla) in proximity to meibomian glands had been initially incorrectly thought to be acinar units.)[11,12] Interestingly in the oral mucosa, rete ridge activation with epithelial cell proliferation has been shown after mechanical stimulation.[12] The mechanical stimulation of gland probing may therefore serve two functions:1) precursor cell activation with epithelial cell proliferation and 2) release of fixed obstructions from periductal fibrosis[13] which may otherwise impair epithelial cell migration proximally within the duct wall.[9,14] This concept is consistent with our previous meibography findings of proximal gland growth, as well as increased gland density and stoutness after meibomian gland probing (MGP).[15]

The relevance and importance of OARREBS was discovered using sequential 2-micron confocal microscopy volume images of MG distal ducts. We found that these OARREBS are in continuity with and may serve a precursor role for MG duct epithelial cells potentially impacting gland health and meibography appearance as well.[10] In this manuscript, we present our data reporting the significant positive impact of MGP on the apparent activation of these OARREBS structures with more superficial and accelerated formation of the distal duct basement membrane plus increased duct wall epithelial cell layers (DWECL), thickness (DWT), and lumen area.

Materials and Methods

Study Design and Patient Selection

For this retrospective observational study, in vivo confocal microscopy (IVCM) volume images taken every 2μm from the central third of upper lids (average of 3 glands/lid) before and after MGP in consecutive patients with obstructive meibomian gland dysfunction (o-MGD) were retrospectively analyzed to identify pre- and post-probing glands, where features and surrounding markings confirmed identical glands. We then followed strict criteria to analyze a very specific cohort that would enable us to confidently study the distal duct microanatomy of Meibomian glands in these patients. These criteria included patients:

- with no previous history of MGP
- that only received MGP with a 76um diameter probe
- with a follow-up maximum of 13 months
- with less than or equal to 12 weeks between initial IVCM and MGP
- whose glands formed a complete and well visualized basement membrane

A cohort of 36 glands from 20 lids of 16 patients (49.24 ±17.11 years old with 13:3 female-to-male ratio) met these criteria and were analyzed. These patients had an average follow-up of 5.03 ±4.48 months post-MGP. For three of the eight analyses in our study, we additionally required optimal IVCM visualization of detailed cellular structures such as duct wall epithelial cell layers, orifice-associated rete ridges, and epithelial cell aggregates. Image quality was affected by technical factors such as slight movement of the eyelid, eye, or head resulting in 31, 30, and 27 gland pairs, respectively for these specific analyses.

We also identified 13 identical gland pairs from 5 lids of 4 patients with obstructive MGD who did not receive MGP to be used as the control group (43.24 ±10.71 years old, all female). The control group had an average follow-up time of 4.69 ±3.68 months. Identical glands were then examined for OARREBS appearance, basement membrane formation, DWECL, distal and proximal DWT, and distal and proximal lumen area. Probed patients may have received additional treatment for comorbid diseases including punctal occlusion, treatment for demodex, and/or ocular surface reconstruction using amniotic membrane. However, no statistically significant difference was found among any measured parameters between patients who received MGP with additional treatment and those who did not. All procedures adhered to the principles of the Declaration of Helsinki. This study received an institutional review board exempt review determination by WCG IRB (Puyallup, WA, USA), an independent institutional review board.

Patient Examinations and Procedures

In Vivo Confocal Microscopy

IVCM was performed using a Heidelberg Retina Tomograph 3 with the Rostock Cornea Module (Heidelberg Engineering, Dossenheim, Germany), which employs a diode laser with a wavelength of 670 nm. Topical anesthesia was achieved using 0.5% proparacaine hydrochloride ophthalmic solution applied to the conjunctival fornix. The microscope lens was covered with a polymethylmethacrylate cap (Tomo-Cap; Heidelberg Engineering GmbH, Dossenheim, Germany) filled with GenTeal Gel (Alcon). Systane Lubricant Eye Ointment (Alcon) was applied to the exterior of the cap. The upper eyelid was everted and the patient was positioned against the chin and head rest. The microscope lens was advanced contacting the lid margin of the patient.

IVCM volumetric Z-scans of the central upper lid margin were performed. These volumetric scans (400µm × 400µm) imaged the glands to a depth of approximately 120µm at intervals of 2µm. The depth was set to zero upon the initial visualization of the superficial epithelial cells. For each lid, an average of 3 consecutive MGs were imaged before MGP and at time of follow-up. As noted above, single glands with surrounding landmarks that confirmed identical matches before and after MGP were selected for the analysis.

Intraductal MGP

MGP was performed as previously described by the first author.[16] The procedure was well tolerated using the following anesthetic protocol: Briefly, one drop of topical 0.5% tetracaine hydrochloride (Bausch and Lomb) was administered to the inferior fornix, followed by placement of a bandage contact lens over the cornea. A topical jojoba anesthetic ointment (JAO) consisting of 8% lidocaine and 25% jojoba in a petrolatum ointment base (compounded at O'Brien Pharmacy, Mission, Kansas, USA) was applied to the inferior lid margin. The eyes were closed for 10 minutes.

An additional drop of topical tetracaine was then placed in the eye and the patient was positioned at the slit lamp. MG orifices were visualized and examined. A 1 mm (used for 29 pairs) and, in some cases, additional probing using a 2 mm (7 pairs) stainless-steel sterile intraductal meibomian gland probe of 76 µm diameter (Katena Products Inc, Denville, NJ, USA) was then inserted into each orifice, perpendicular to the lid margin using a dart throwing motion. The location and angle of the probe were adjusted as needed to achieve the proper angle of entry. Frequent "pops and gritty sounds" were audible as periductal fibroses (PDF) were released, and resistance gave way allowing the probe to freely pass to and fro within the duct. Once inside the distal duct of the gland, a brief circular motion of the probe was used to debride the suprabasal epithelium and dilate the lumen. Statistical analysis was performed which showed no significant difference in the results for all parameters in this study when comparing cases using the 1 mm probe to cases receiving an additional 2 mm probing.

Data Collection and Analysis

IVCM Image Analysis

Progressive volumetric Z-scans were used for analysis to visualize morphologic and cellular changes during the formation of the Meibomian gland duct wall, including appearance of a well-defined lumen with surrounding epithelial cell layers, and a basement membrane with an associated basal epithelial cell layer.

Landmarks surrounding the MGs were used to identify identical glands for pre- and post-MGP analysis. The depth of the rete ridge was defined as the depth of the greatest rete ridge clarity (Figure 1B). This was deeper than the initial non-

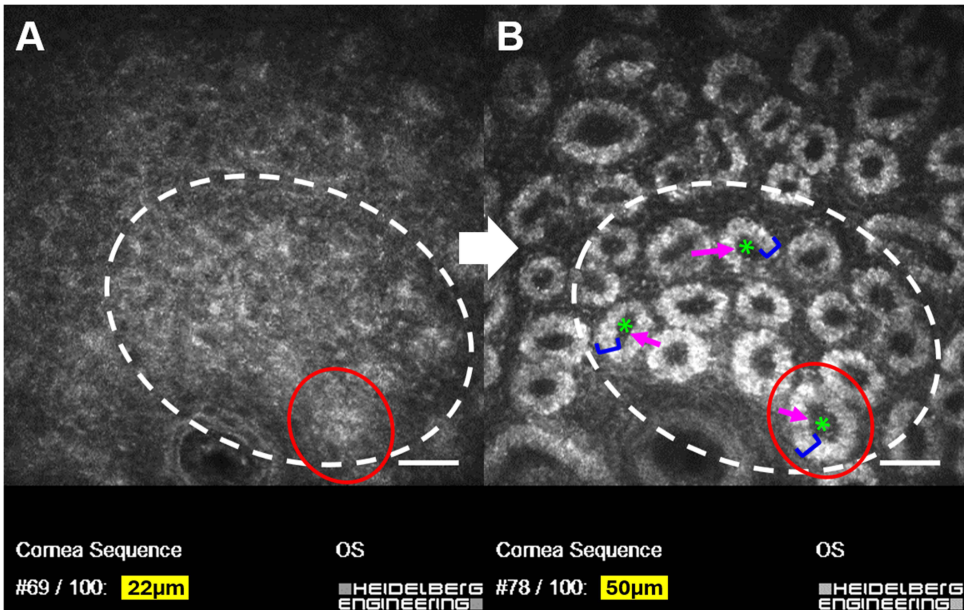

Figure 1 Image of rete ridges at the lid margin of an upper lid using in vivo *confocal microscopy* (IVCM). (**A**) Superficial epithelial cell aggregates which organize into orifice-associated rete ridge epithelial/basement membrane structures (OARREBS) with increased depth. (**B**) At a greater depth, each rete ridge has a bright outer epithelial cell layer (blue bracket), a dark center dermal component (green asterisk), and a junctional basement membrane that resides between these two (pink arrow).[11,12] White dashed circle denotes the area of interest while red circle highlights a single rete ridge from the progression of epithelial cell aggregate (**A**) to complete rete ridge formation (**B**) as the depth increases. Scale bar, 50µm.

focused appearance of epithelial aggregates (Figure 1A) and superficial to the depth where rete ridges ultimately flattened and become continuous with the basement membrane and basal epithelium. The depth of the basement membrane formation was recorded at the initial most superficial depth of the complete 360° well-demarcated basement membrane. The depth of initial epithelial aggregate visualization was subtracted from the depth of complete basement membrane formation to indicate the velocity of the rete ridge to basement membrane formation.

The number of pre-MGP DWECL was measured at the depth of the initial complete basement membrane formation found during pre-MGP analysis using the ImageJ pointer tool. For the post-MGP DWECL, the same depth was used as for the pre-MGP analysis. Starting at 12 o'clock on the lumen, the DWECL was counted along a straight line moving away from the lumen and extending to the basement membrane at 12 o'clock. MGs that did not have the resolution to observe individual epithelial cells were excluded from analysis.

To measure and compare the changes in DWT and lumen area, ImageJ was used to outline the basement membrane and lumen area. The lumen area was subtracted from the area within the basement membrane to determine DWT (μm^2). The initial most superficial depth from the pre-MGP IVCM, demonstrating complete 360° well-demarcated basement membrane formation, was used for analysis. This depth was used for the distal DWT and lumen area and was measured at an average depth of 83.81µm. Measurements were then taken at the same depth for post-MGP distal DWT and lumen area analyses. (Typically, the basement membrane of the MG post-MGP is formed at a more superficial depth than that of the pre-MGP. To be consistent, pre-MGP depth measurement was used to evaluate the effect of MGP on the distal DWT and lumen area.) Proximal DWT and lumen area was determined at the last depth proximally that the complete basement membrane of both pre and post-MGP MGs was clearly demarcated and was measured at an average depth of 105.19µm.

Statistical Analysis

Statistical significance was set at $p < 0.05$. The effect of MGP on all quantifications was analyzed by nonparametric *t*-tests. We used a Wilcoxon Signed Rank test for all of the tested pre-MGP vs post-MGP parameters of the test group, and a Mann Whitney *U*-test for all parameters comparing test vs control group. All statistical analysis was performed in IBM SPSS version 27.

Results

Rete Ridge Structures are in Continuity with Meibomian Gland Distal Basement Membrane

Upon reviewing progressive volume IVCM scans, we observed the basement membrane of the epidermal-dermal junction of lid margin orifice-associated rete ridges[11] to be in continuity with the meibomian gland distal duct basement membrane. On IVCM, these rete ridges first appear as epithelial cell aggregates (Figure 1A). With further depth, these rete ridges fully reveal their ring structure (Figure 1B), then with further depth ovalize and flatten, allowing each ridge to increase its arc around the perimeter of the distal duct as it coalesces with adjacent rete ridges to connect to and possibly form a well-demarcated basement membrane and basal epithelial layer (Figure 2).[10,11]

Rete Ridge Epithelial Cells are in Continuity with Meibomian Gland Duct Wall Basal Epithelial Cell Layer

While the epidermal-dermal basement membrane of the rete ridges is in continuity with the MG basement membrane, the epithelial cell component of the rete ridges appears to be in continuity with the ductal basal epithelial cell layer. As these rete

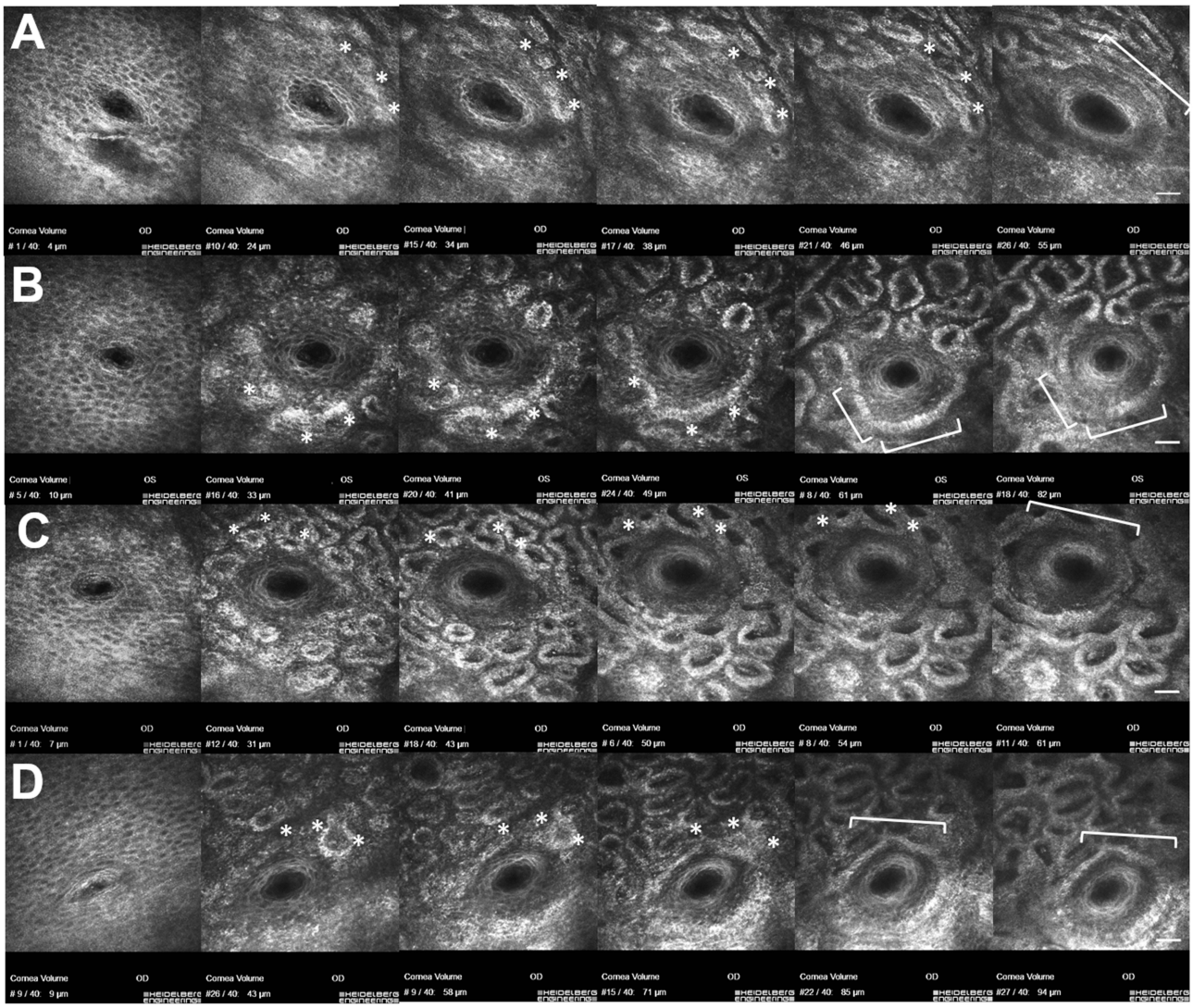

Figure 2 Images of progressive volumetric scans of lid margin rete ridges in continuity with Meibomian gland basement membrane and basal epithelium using in vivo confocal microscopy (IVCM). Each meibomian gland orifice (**A**–**D**) demonstrates individual orifice associated rete ridges in peri-lumenal position (white asterisks) ovalize, flatten, and appear to coalesce with adjacent rete ridges to form the Meibomian gland basement membrane and ductal basal epithelium with increased depth (white bracket). Scale bar, 50μm.

ridges undergo morphologic changes and appear to coalesce with adjacent rete ridges, their combined epithelial components seemingly connect to or organize into a continuous basal epithelial cell layer that lines the basement membrane.[10,15,17]

During the review of IVCM images of pre- and post-MGP identical MG pairs, we also observed orifice-associated rete ridges post-MGP spawning epithelial cells to the duct wall (Figure 3). In this figure, the pre-MGP orifice-associated rete ridges appear in continuity with the MG basement membrane and basal epithelial complex, as described above (Figure 3A). However, the identical gland orifice-associated rete ridges post-MGP clearly showed a single epithelial cell cleaved from the orifice-associated rete ridges and incorporated into the MG duct wall epithelial cell layers as the remaining smaller orifice-associated rete ridge structure was noted, with increased depth, to be further from the MG lumen forming a portion of the basement membrane (Figure 3B). Additionally, it should be noted that the OARREBS in the post-MGP gland begin this process at a more superficial depth than the pre-MGP gland, consistent with the findings of this study (see next Results section "More Superficial Rete Ridge Appearance Post-MGP"). Figure 3C–E show representative pre-and immediate post-probing IVCM of the distal duct, confirming the probe placement track was

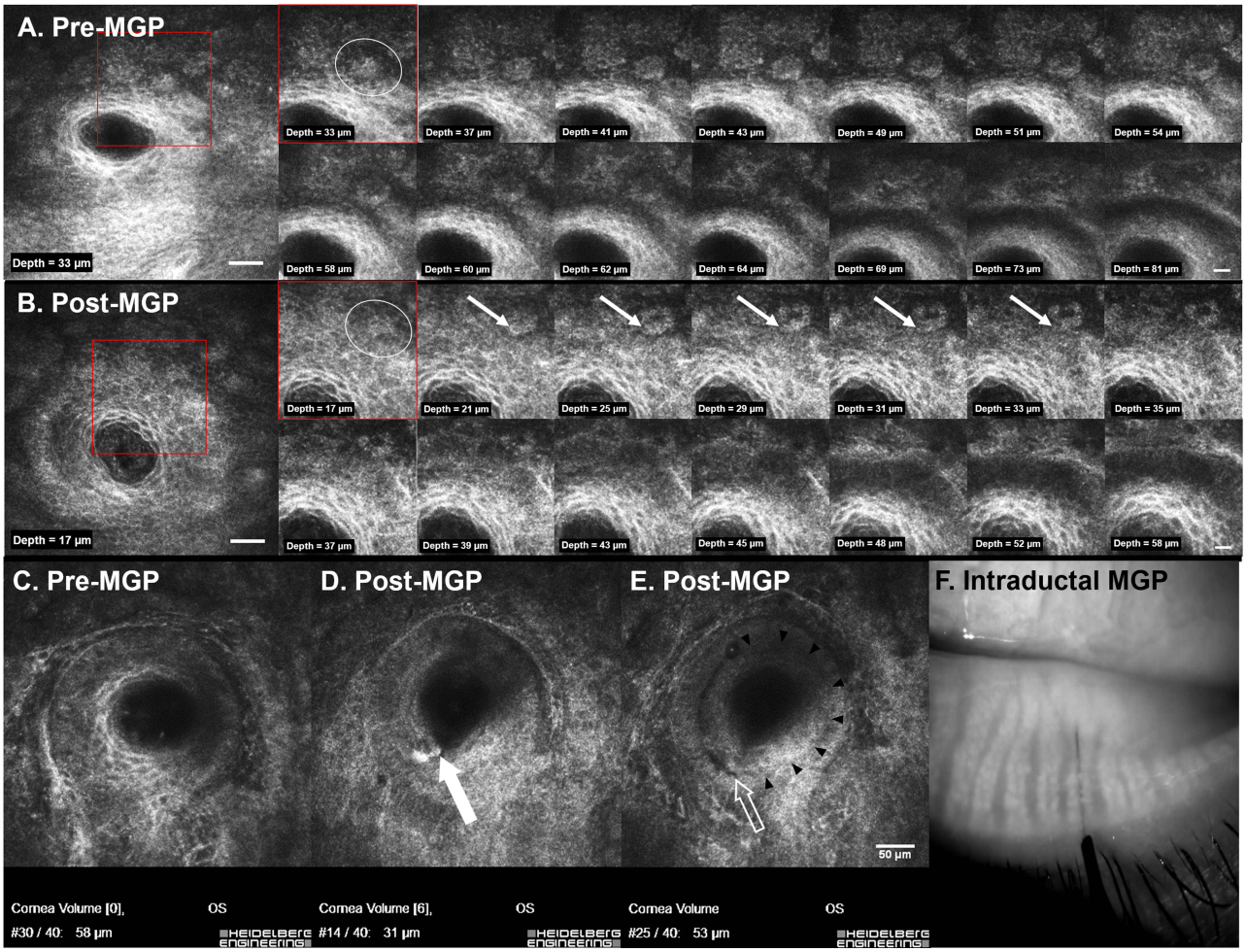

Figure 3 (**A** and **B**) Images of progressive volumetric scans of an identical gland pre and post-Meibomian gland probing (MGP) using in vivo confocal microscopy (IVCM). Red outline indicates inlay of larger image. (**A**) Meibomian gland pre-MGP showing orifice-associated rete ridge epithelial/basement membrane structures (OARREBS) (white circle) in continuity with the basement membrane and basal epithelium of the Meibomian gland. (**B**) Identical Meibomian gland to (**A**) post-MGP showing the same OARREBS (white circle) with a single epithelial cell (white arrow) cleaving from the OARREBS and incorporating into the Meibomian gland duct wall epithelial cell layers. The remaining smaller OARREBS is further from the Meibomian gland lumen with subsequent morphologic change into a portion of the basement membrane. Large image scale bar, 50µm; small image scale bar, 20µm. (**C**–**E**) IVCM images immediately before and after MGP using a 76µm probe. (**C**) Meibomian gland immediately pre-MGP. (**D** and **E**) Meibomian gland immediately post MGP at a depth of 31µm and 53µm, both showing a notch at the lumen inferiorly. Image (**D**) demonstrates apparent debridement of terminally differentiated and keratinized epithelium lining the lumen while (**E**) shows probe path through suprabasal ductal epithelium. Probing procedure is confined to the epithelium compartment, explaining lack of secondary fibrosis. (**F**) Location and presence of a 4mm length probe (76µm OD) inside the duct of a meibomian gland using infrared video meibography. Note that acinar-ductule units are visible overlying the device. (**F**) adapted with permissions from Maskin, Steven L., and Sreevardhan Alluri. "Meibography guided intraductal meibomian gland probing using real-time infrared video feed". British Journal of Ophthalmology 104.12 (2020): 1676–1682.

confined within the duct epithelial compartment. Figure 3F reproduced from our previous published study in *British Journal of Ophthalmology* further supports the location of the probing device (4 mm, 76µm OD) within the central duct of a meibomian gland using video meibography. Note that the acinar-ductule units are visible overlying the device.[17]

More Superficial Rete Ridge Appearance Post-MGP

IVCM volumetric images of 36 identical pre-MGP and post-MGP MG pairs were examined to determine the depth at which the clearest orifice-associated rete ridges were observed. Of these 36 MG pairs, six were excluded because of a lack of visible orifice-associated rete ridges (in one case) or insufficient resolution to clearly visualize them for analysis (in five cases). The remaining 30 gland pairs from 18 lids of 14 patients with an average follow-up of 3.91 ±3.61 months were considered. Statistical analysis showed a significant difference in depth for clear observation of RR from 45.67 ±8.57µm pre-MGP to 37.73 ±8.98µm post-MGP, with an average of 17.13% more superficial appearance ($p = <0.001$) (Figure 4A). This change was statistically different from that observed in the control group ($p = 0.010$).

More Superficial Formation of Basement Membrane Post-MGP

All 36 identical pre-MGP and post-MGP MG pairs showed complete basement membrane formation within the first 110µm of the IVCM volumetric scan. The most superficial depth of complete 360° basement membrane formation for each MG was recorded. Statistical analysis showed a significant difference in depth of basement membrane formation

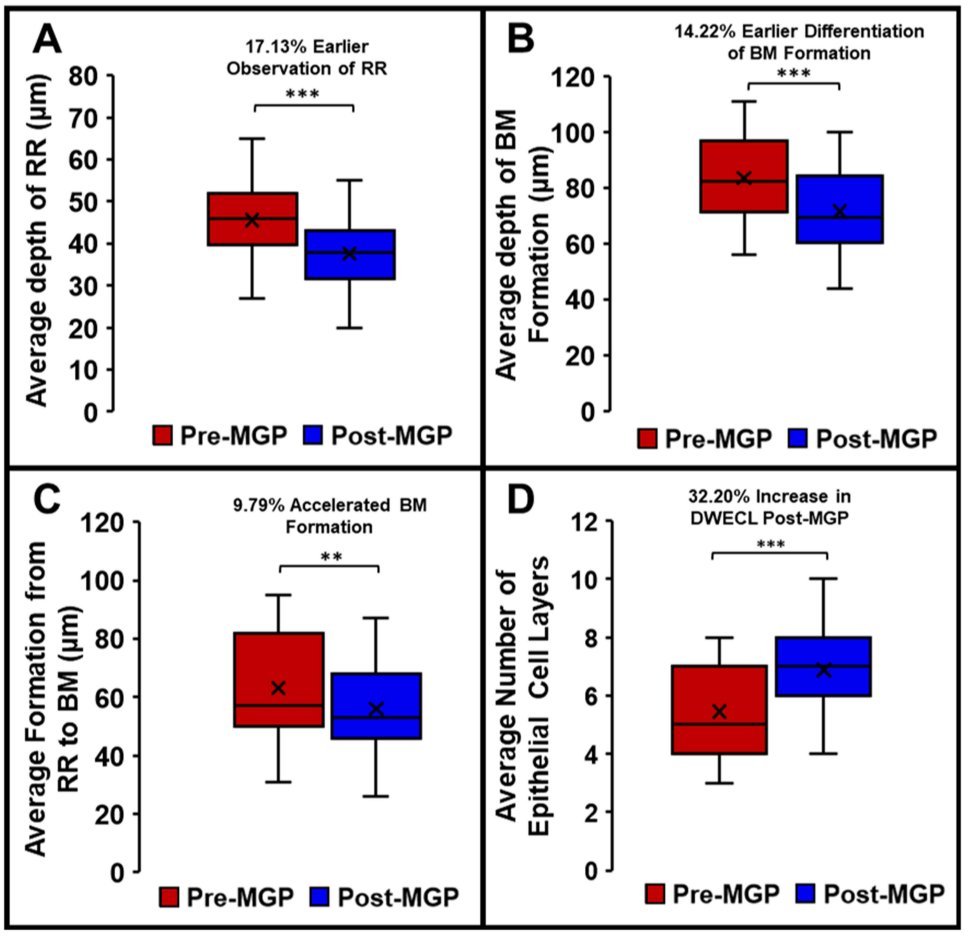

Figure 4 Graphs demonstrating the change in each parameter from pre-Meibomian gland probing (MGP) (red) to post-MGP (blue). (**A**) Meibomian glands show an average of 17.13% more superficial appearance of rete ridges post-MGP ($t(30)=4.597$, $p<0.001$). (**B**) Meibomian glands had an average of 14.22% earlier basement membrane formation post-MGP ($t(36)=5.03$, $p<0.001$). (**C**) Meibomian glands demonstrate an average acceleration compared to baseline of 9.79% from rete ridges (RR) to basement membrane (BM) post-MGP ($t(27)=3.97$, $p=0.002$). (**D**) Meibomian glands had an average increase in duct wall epithelial cell layers (DWECL) of 32.20% post-MGP ($t(31)=4.68$, $p=<0.001$). (**$p<0.01$, ***$p<0.001$).

from 83.47 ±14.25 µm pre-MGP to 71.50 ± 14.85µm post-MGP, with an average of 14.22% more superficial formation (p = <0.001) (Figure 4B). This change was statistically different from that observed in the control group (p = <0.001).

Accelerated Basement Membrane Formation Post-MGP

The 36 identical pre-MGP and post-MGP MG pairs were evaluated to determine the depth extending from the initial appearance of epithelial aggregates to complete basement membrane formation. Of these, six pairs were excluded due to a lack of RR present (in one case) or insufficient image quality to analyze them (in 5 cases), with an additional three pairs excluded due to incomplete lid contact during the beginning of the scan preventing clear visualization of initial rete ridge aggregates. The remaining 27 MGP pairs from 16 lids of 14 patients with an average follow-up of 3.97 ±3.54 months were considered. Epithelial aggregates were observed before probing at an average depth of 21µm while after probing at an average depth of 16µm. The depth of the initial aggregate observation was subtracted from the depth of the complete basement membrane formation. Statistical analysis showed a significant difference in distance from epithelial aggregates to basement membrane formation from 63.04 ±17.48µm pre-MGP to 56.04 ±15.49µm post-MG, an average acceleration compared to baseline of 9.79% (p = 0.002) (Figure 4C). This change was statistically different from that observed in the control group (p = 0.007).

Increase of Duct Wall Epithelial Cell Layers (DWECL) Post-MGP

IVCM images of 36 identical pre-MGP and post-MGP MG pairs were evaluated to determine the changes in the number of duct wall epithelial cell layers (DWECL). Of these, five cases were excluded because of image quality insufficient in enabling us to observe each cell. The remaining 31 MG pairs from 18 lids of 16 patients with an average follow-up of 4.68 ±4.40 months were measured. Statistical analysis showed a significant increase in DWECL from 5.45 ±1.93 cell layers pre-MGP to 6.87 ±1.84 layers post-MGP, with a mean of the average increases of 32.20% (p = <0.001). This change was statistically different from that observed in the control group (p = <0.001) (Figure 4D).

Increased Distal and Proximal Duct Wall Thickness (DWT) with Lumen Dilation Post-MGP

Using IVCM, 36 identical pre-MGP and post-MGP MG pairs were measured to determine changes in duct wall thickness and lumen both distally and proximally. For distal measurements, the initial most superficial depth from the pre-MGP IVCM, demonstrating a complete 360° well-demarcated basement membrane formation, was used for analysis. This depth was defined as the distal DWT and lumen area and was measured at an average depth of 83.81µm. Statistical analysis showed a significant increase in distal DWT from 35,872.75 ± 9324.51µm^2 pre-MGP to 44,289.38 ± 10,336.53µm^2 post-MGP, an average increase of 25.40% (p = <0.001). This change was statistically different from that observed in the control group (p = <0.001). In addition, statistical analysis also revealed a significant increase in distal lumen area from 3361.39 ± 1199.23µm^2 pre-MGP to 5225.66 ± 2426.11µm^2 post-MGP, an average increase of 77.74% (p = <0.001) (Figure 5A). This difference was also statistically different from that in the control group (p = 0.037).

Of these 36 cases, the basement membrane of 30 MG pairs continued proximally with good image clarity. The proximal DWT and lumen area were determined as the last depth proximally that the complete basement membrane of both pre- and post-MGP MGs was clearly demarcated and measured at an average depth of 105.19µm. Statistical analysis showed an increase in proximal DWT from 36,004.69 ±8613.70µm^2 pre-MGP to 46,531.91 ±9024.68µm^2 post-MGP, an average increase of 32.04% (p = <0.001). This change was statistically different from that observed in the control group (p = <0.001). The increasing lumen area also continued proximally, with a statistically significant increase from 3971.26 ± 1541.99µm^2 pre-MGP to 6471.59 ± 2567.18µm^2 post-MGP, with an average increase of 81.34% (p = <0.001) (Figure 5B). This change was significantly different from that observed in the control group (p = 0.007). There was no significant difference between the increase in DWT proximally and distally (p = 0.170), or the increase in lumen area proximally compared to that distally (p = 0.710).

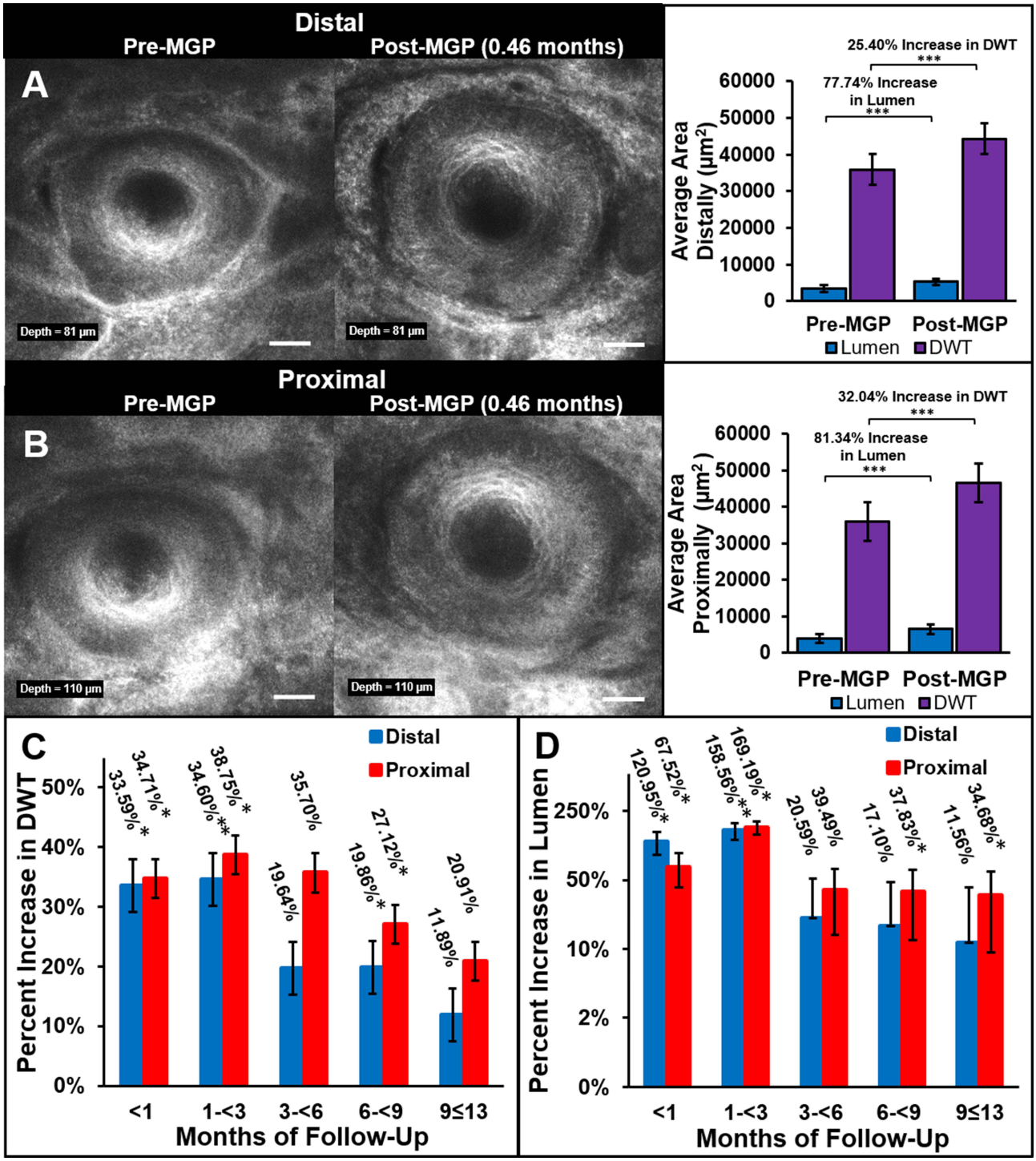

Figure 5 (**A**) Representative in vivo confocal microscopy (IVCM) images of an identical Meibomian gland at a depth of 81µm pre and post-Meibomian gland probing (MGP). This example is 0.46 months post-MGP. Statistical analysis revealed a significant 25.40% average increase in distal duct wall thickness (DWT) (purple) post-MGP (t(36)=5.035, p<0.001) and a significant 77.74% average increase in distal lumen area (blue) post-MGP (t(36)=5.035, p<0.001). (**B**) Representative IVCM images of the same identical Meibomian gland as "A" at a depth of 110µm pre and post-MGP. Statistical analysis revealed a significant 32.04% average increase in proximal DWT (purple) post-MGP (t(30)=4.597, p<0.001) and a significant 81.34% average increase in proximal lumen area (blue) post-MGP (t(30)=4.597, p<0.001). (**C**) Average percent increase in distal (blue) and proximal (red) DWT post-MGP over time (months). When compared to baseline, glands with a less than 1 month, 1 month or greater and less than 3 months, 3 months or greater and less than 6 months, 6 months or greater and less than 9 months, 9 months or greater and less than or equal to 13 months follow-up had an average increase in distal DWT of 33.59% (n=9, p=0.015), 34.60% (n=9, p=0.008), 19.64% (n=4, p=0.068), 19.86% (n=7, p= 0.028) and 11.89% (n=7, p=0.063), respectively, and an average increase in proximal DWT of 34.71% (n=9, p=0.011), 38.75% (n=8, p=0.012), 35.70% (n=2, p=0.180), 27.12% (n=6, p=0.028), and 20.91% (n=5, p=0.080), respectively. (**D**) Average percent increase in distal (blue) and proximal (red) lumen area post-MGP over time (months). When compared to baseline, glands with a less than 1 month, 1 month or greater and less than 3 months, 3 months or greater and less than 6 months, 6 months or greater and less than 9 months, 9 months or greater and less than or equal to 13 months follow-up had an increase in distal lumen area of 120.95% (n=9, p=0.011), 158.56% (n=9, p=0.008), 20.59% (n=4, p=0.273), 17.10% (n=7, p=0.128), and 11.56% (n=7, p=0.237), respectively, and an increase in proximal lumen area of 67.52% (n=9, p=0.021), 169.19% (n=8, p=0.017), 39.49% (n=2, p=0.180), 37.83% (n=6, p=0.028), and 34.68% (n=5, p=0.043), respectively. Scale bar, 50µm. (*p<0.05, **p<0.01, ***p<0.001).

https://doi.org/10.2147/OPTH.S452549 DovePress

Increased Duct Wall Thickness (DWT) and Lumen Dilation Post-MGP Over Time

The increase in distal and proximal DWT showed a significant and trending negative correlation respectively with the number of months of follow-up post-MGP (significant at p = 0.004 and trend at p = 0.084, respectively) (Figure 5C). When compared to baseline, glands with a less than 1 month, 1 month or greater and less than 3 months, 3 months or greater and less than 6 months, 6 months or greater and less than 9 months, 9 months or greater and less than or equal to 13 months follow-up had an average increase in distal DWT of 33.59% (n = 9, p = 0.015), 34.60% (n = 9, p = 0.008), 19.64% (n = 4, p = 0.068 trend), 19.86% (n = 7, p = 0.028) and 11.89% (n = 7, p = 0.063 trend), respectively, and an increase in proximal DWT of 34.71% (n = 9, p = 0.011), 38.75% (n = 8, p = 0.012), 35.70% (n = 2, p = 0.180 low n), 27.12% (n = 6, p = 0.028), and 20.91% (n = 5, p = 0.080 trend), respectively.

The increase in distal and proximal lumen areas also showed a significant and trending negative correlation respectively with the months of follow-up post-MGP (significant at p = 0.010 and trend at p = 0.066, respectively) (Figure 5D). When compared to baseline, glands with a less than 1 month, 1 month or greater and less than 3 months, 3 months or greater and less than 6 months, 6 months or greater and less than 9 months, 9 months or greater and less than or equal to 13 months follow-up had an average increase in distal lumen area of 120.95% (n = 9, p = 0.011), 158.56% (n = 9, p = 0.008), 20.59% (n = 4, p = 0.273), 17.10% (n = 7, p = 0.128), and 11.56% (n = 7, p = 0.237), respectively, and an increase in proximal lumen area of 67.52% (n = 9, p = 0.021), 169.19% (n = 8, p = 0.017), 39.49% (n = 2, p = 0.180 low n), 37.83% (n = 6, p = 0.028), and 34.68% (n = 5, p = 0.043), respectively.

Discussion

Obstructive meibomian gland dysfunction is considered to be the most common factor in Dry Eye Disease and has traditionally been frustrating to manage. The frustration in managing this disease has been greatly overcome with the discovery and treatment of the fixed intraductal obstruction(s) found in over 90% of glands in lids with MGD.[13] The existence of fixed intraductal obstruction is thought to be secondary to periductal fibrosis (PDF). These fibrotic bands wrapped around the duct wall can be released with intraductal probing which in turn has led to an increase of gland tissue, as seen on meibography,[15] as well as increasing numbers of functional glands while reducing lid tenderness and improving symptoms excluding lid tendernesss.[16] The global literature including five randomized control trials[18–22] has been reviewed[23] and showed significant improvement in subjective and objective clinical parameters of patient comfort and gland function after MGP for patients refractory to previous treatments, and against control groups of sham probing, topical steroid, conventional therapy and intense pulse light therapy (IPL).[18–22]

The success of MGP in treating obstructive MGD was largely due to the specific targeting and release of uni and multifocal fixed fibrotic obstructions.[13] The mechanical release of fibrotic bands equilibrated intraductal pressure on either side of the obstruction with immediate and dramatic reduction in lid tenderness. We have also previously reported increased gland tissue and reduction in symptoms *excluding lid tenderness* such as burning and photophobia after probing, and have previously suggested that these findings may be due in part to the activation of gland stem cells with improved gland function.[3,15,16,24] In this present study, we provide evidence supporting the concept that MGP stimulates a proliferative epithelial response, suggesting the activation of lid margin meibomian gland precursor cells, a conclusion supported by findings at the *cellular level* using confocal microscopy and analogous to the mechanical stimulation of the oral mucosa which was shown to stimulate epithelial proliferation via rete ridge activation.[12] In our study, confocal microscopy findings revealed lid margin orifice-associated rete ridge structures are in continuity with MG distal duct BM and basal epithelial cell layers and therefore may play a fundamental role in the formation of the MG ductal compartment and would be consistent with Krox20 genetic study.[9,14] Furthermore, that MGP stimulated a proliferative epithelial response characterized by accelerated formation of the ductal basement membrane with increased DWECL, DWT, and lumen area at two separate duct foci. Control glands that had not been probed showed no significant change in distal duct microanatomy over a similar follow-up period.

At ARVO 2022, using confocal microscopy volume studies, we first reported the concept of OARREBS possibly serving as MG ductal precursor cells as it was observed to be in continuity with and therefore possibly differentiate into MG ductal basement membrane and basal epithelium.[10] Figure 2 shows four examples of healthy OARREBS in

continuity with MG ductal basal epithelium and basement membrane in glands that have not been probed. After MGP, epithelial cell aggregates (Figure 1A) destined to organize into OARREBS (Figure 1B) appeared, on average, at a more superficial (16μm instead of 21μm) depth post-probing. This led to statistically significant accelerated and more superficial formation of the MG ductal basement membrane.

As the mechanical stimulation of gland probing led to an earlier, more superficially organized OARREBS, there was a corresponding robust epithelial cell proliferation with increased ductal cell layers and increased DWT. It is worth noting that this cellular response to gland probing extended through the greatest depth allowed by confocal imaging as statistically significant changes occurred both distally (83.81μm) at the depth where a complete basement membrane was first formed and proximally (105.19μm) before image clarity was lost. It should also be noted that during this proliferative response within the ductal epithelium, the lumenal area was preserved and enlarged. This finding of increased lumen capacity suggests that mechanical pressure emanating from the rapid expansion of increased epithelial cell density[9,14] extends centrifugally and proximally while respecting the intralumenal space. Maintenance of intraductal pressure from meibum flow through the newly restored ductal outflow tract may support lumen integrity and retain its new dimensions. The other possibility of increased duct wall thickness and cell layers from proliferation of pre-existing ductal epithelial cells is less likely, as we have seen cases of glands without OARREBS showing an intact but significantly less proliferative response (personal observation).

It is interesting that in all cases, there was a limit on the increase in DWT to approximately 35% (at 1-<3 months) suggesting that centrifugal pressure may be limited by the original basement membrane and periductal connective tissue, driving the growth and migration of daughter cells proximally deeper into the gland, perhaps explaining the finding of increased gland tissue on meibography in over 41% of probed lids with MGD.[15] Table 1 from this 2018 study showed 10 of the 14 (71%) lids with signs of increased gland tissue characterized by increased gland density and stoutness consistent with our cytologic findings of increased DWT and DWECL. Additionally, six of the 14 (43%) lids showed proximal gland lengthening. This proximal growth, as well as increased gland density and stoutness, was consistent with concepts recently reported in a mouse study demonstrating that the KROX20 gene marks a stem/progenitor cell population that differentiates to form the entire adult MG from the lid margin proximally, including the distal and proximal ducts, and acini.[9] This further suggests the possibility that stem cells differentiate at the lid margin into daughter cells that migrate proximally within the duct wall and may explain the proximal gland lengthening that we have previously reported.[9,15]

The role of OARREBS now seems apparent as it relates to the MG. In addition, although it is well known that lid margin health and location of vital staining of the mucocutaneous junction correlate with MG function and atrophy as seen on meibography[25–27] it is now suggested that the key link between lid margin health and meibography results is the OARREBS status (unpublished data). Furthermore, it appears that the health or dysfunction of OARREBS helps to maintain and preserve or fail to support MG tissue, respectively (unpublished data). Maintenance of healthy OARREBS is of paramount importance and underscores the significance of a healthy lid margin and tear film, which could otherwise individually and together compromise OARREBS health and function. The important role of OARREBS in the maintenance of MG tissue suggests that while lid margin hygiene is necessary for OARREBS health, aggressive exfoliative procedures focused along the lid margin may introduce iatrogenic injury to these structures.

The notion that mechanical treatment can activate epithelial precursor cells is well established within Ophthalmology and specifically within the Cornea and External Disease subspecialty.[28,29] The findings in this current study may be analogous to the activation effect from de-epithelializing the cornea such as the therapeutic debridement of map-dot-fingerprint corneal epithelial dystrophy,[30] Salzmann's nodular degeneration,[31] or the margins of a corneal persistent epithelial defect with activation of limbal precursor and transient amplifying cells (TAC) to proliferate and close the defect.[29] These TACs can migrate more than 5 mm to the central cornea.[32] This current study appears to show an analogous pattern where MG orifice-associated rete ridges may be activated by MGP inducing a proliferative response with increased DWECL and DWT distally which extends proximally. This suggests that proliferating ductal epithelium can migrate within the duct wall, creating growth pressure toward the proximal end of the duct, thereby increasing gland tissue.[9,14]

Interestingly, the typical length of the healthy upper lid meibomian glands at approximately 5 mm is similar to the distance travelled by limbal-derived TACs reaching the central cornea.[32] Thus, the mechanical action of gland probing appears to have a salutary effect on gland health, acting both proximally on PDF and distally on OARREBS. While the act of probing can release the PDF for the entire length of the probe, thereby reducing resistance within the duct wall to migrating epithelial cells, there is a concomitant growth-promoting effect on the distal duct likely mediated by OARREBS, which may extend proximally to the full length of the gland probing. Furthermore, the analogy to corneal limbal stem cells is also consistent in the setting of stem cell deficiency leading to reduced proliferative potential, increased inflammation, fibrovascular proliferation, and conjunctivalization into the peripheral cornea.[32] We see a similar pattern with MG orifices characterized by unhealthy associated rete ridges (eg poorly demarcated, enlarged or reduced size, thin epithelium and/or tapered in shape with dermal inflammation) showing increased periductal fibrosis and increased fibrovascular activity in the periductal tissues (personal observation), demonstrating circumferential constriction of the distal duct with lumen stricture as well as focal disruption of the basal epithelium and basement membrane as imaged with IVCM.[13]

The results reported here underscore the regenerative capacity of the meibomian gland. As an ectodermal derivative, along with other ectodermal derivative epithelial systems, such as limbus/cornea, sebaceous gland/hair follicle, and other glands, including salivary and mammary glands,[33] MG retains the ability to regenerate the ductal compartment when stimulated by gland probing. This raises questions as to the etiology of the decreased duct wall epithelial cell layers reported in patients with MGD.[3] Perhaps the reduction of ductal epithelial layers is secondary to OARREBS deficiency or increased duct wall "back pressure" caused by the constriction effect of periductal fibrosis blocking cellular migration proximally, or both. Notably, the therapeutic effect of probing with increased DWECL and DWT are of a pure epithelial regenerative response. Images of MG orifices immediately post-probing showed that the passage of the probe was restricted to the epithelial ductal compartment (Figure 3C and D) indicating that probing initiates a direct mechanical intraductal stimulus through debridement of the suprabasal, senescent and keratinized ductal epithelium, which could activate the proliferation of stem cell-induced transient amplifying daughter cells.[15,16] There was no post-probing fibroblast activation or increase in scar tissue noted in the extraglandular connective tissue. No adverse effects on MG anatomy have been reported using IVCM and meibography.[22,34,35]

Figure 5A and B show the study data as well as examples of pre- and post-MGP (0.46 months) duct wall and lumen from two foci of the same gland along the distal duct, revealing significantly increased DWT while maintaining and significantly increasing lumen area. Figure 5C and D shows the effects of MGP over 13 months on these parameters. As shown in Figure 5C, the significant increases in DWT were similar for the first month for both distal (33.59%, $p = 0.015$) and proximal (34.71%, $p = 0.011$) foci, further increasing and maintaining significance to 34.60% ($p = 0.008$) and 38.75% ($p = 0.012$), respectively, between 1 and less than 3 months, showing a reduction of this increase for the 3-<6 (distal $p = 0.068$ showing trend, proximal $p = 0.180$ with $n = 2$ not significant), 6-<9 (distal $p = 0.028$ and proximal $p = 0.028$, both significant), and 9 < 13 months still showed a trend of 11.89% ($p = 0.063$) and 20.91% ($p = 0.080$) increased distal and proximal DWT, respectively. This year-long increase in DWT is consistent with the established clinical response to probing, where the improvement in symptoms peaked at approximately 3–6 months with continued improvement extending for 8–12 months.[24] It is interesting that at each time point, the increase in DWT for the proximal foci exceeded that of the distal foci and may be related to the effects of the tear film or superficial lid margin disease affecting the most distal duct tissue, thus reducing its proliferative OARREBS response with a trailing response proximally perhaps similar to how signs of limbal deficiency with abnormal vital staining first appear peripherally and then extends centrally.[36]

Figure 5D shows a significant increase over baseline in the duct lumen area at <1 month of 120.95% (distal, $p = 0.011$) and 67.52% (proximal, $p = 0.021$). A greater initial increase in the distal lumen may reflect the enhanced dilating effect of locating the correct angle for entering the orifice lumen at the lid margin. At 1-<3 months, the proximal lumen showed an increase in area to a greater percentage than the distal lumen (169.19%, $p = 0.017$ versus 158.56%, $p = 0.008$, both significant), and then lost significance at 3-<6 months ($p = 0.180$, low n). The proximal lumen at 6-<9 months ($p = 0.028$) and at the end of the study at 9-<13 months ($p = 0.043$) maintained a significantly increased area of >34%, while the distal lumen area decreased to a non-significant increase over baseline with an increase of 20.59% at 3-<6 months

(p = 0.273), gradually decreasing further to 17.10% (p = 0.128) and 11.56% (p = 0.237) by 13 months. This result may reflect the adverse impact of tear film and lid margin disease, which may have impacted the gradual reduction in DWT during the course of the year.

While it is understandable that the reduction in the significance or trend of the increase in DWT and lumen area for distal foci was reduced during the course of 13 months post-MGP (with lumen measurements losing significance at 3-<6 months), the increase remained above baseline by more than 11% throughout the study. It is also remarkable that the increase in proximal DWT and lumen remains greater than that of the distal duct, with levels of over 20% increased DWT and over 34% lumen area at 13 months post-probing. Thus, we observed the residual therapeutic effect of MGP at the cellular level at one year. It is possible that the effect of MGP on these two (distal and proximal) foci of the distal duct may also occur deeper within the gland along the extended proximal duct, as the growth pressure of the proliferative duct wall epithelium is no longer blocked by the constrictive effects of periductal fibrosis. This observation may explain the findings of increased gland tissue proximally, as seen on meibography[15] consistent with gland regeneration in the ductal compartment.

Interestingly, until the relatively recent description of the proximate cause of obstructive MGD as periductal fibrosis and its targeted release using MGP, its treatment was palliative and non-specific, leading to inconsistent and unsatisfactory results. Palliative treatments include the use of artificial tears, most recently lipid-based tear replacement drops, as well as heat (warm compresses) and pressure (therapeutic expression and massage) in an attempt to thin and push gland secretions out through the natural orifice. These palliative treatments have more recently included device approaches such as Lipiflow, I-lux, and Tear Care. Other palliative measures include treatment of comorbidities such as aqueous tear deficiency (ATD), allergy, and anterior blepharitis. Non-specific and therefore non-targeted approaches to reduce inflammation associated with gland obstruction and comorbid diseases include devices such as IPL, which is thought to lead to thrombosis of lid margin vessels to reduce inflammation but does not target periductal fibrosis.[37] Typically, IPL is also followed by therapeutic expression, which together may increase intraductal pressure and exacerbate symptoms.[19,37] Other non-specific treatments include omega 3 fatty acids and oral antibiotics such as lipophilic doxycycline, which may act within the lid as an oxygen radical scavenger, and topical corticosteroids.

Limitations of this study include its retrospective design and sample size. There is a lack of a marker tool to confirm that each pre- and post-MGP glands are identical. However, by using surrounding landmarks and detailed study, we only included glands that we could confidently match. Using multiple glands from the same lid or more than one lid of the same patients may introduce bias; however, the retrospective review of IVCM in patients pre- and post-MGP where identical glands were identified was random, and all glands that met our criteria for this study were included. It may be possible for some reason, multiple glands of the same patient may respond in a uniquely similar way. However, in a separate analysis, for patients that had more than one gland per lid, or more than one lid included in the study, we averaged all measures to result in one value for each parameter. In all cases, results remained significant when comparing pre-MGP to post-MGP changes on IVCM (n = 16).

The results of this study demonstrated that MGP is a targeted therapy that stimulates a direct response within the distal ductal epithelium of the meibomian gland, characterized by accelerated formation of the ductal basement membrane with increased DWECL and DWT at two separate duct foci while retaining and increasing lumenal capacity. Together, this suggests the activation and proliferation of lid margin meibomian gland duct precursor epithelial cells and confirms that MGP stimulates an epithelial regenerative phenomenon, not fibrosis.

Conclusion

The concept of existence and localization of MG ductal precursor cells within the orifice-associated rete ridges of the posterior lid margin as suggested in this manuscript is novel, significant, and has important clinical implications. These implications are derived from the impact of this concept on the diagnosis, treatment, and prognosis of obstructive MGD. In this context, MGP is an important therapy for targeting and releasing constricting periductal fibrosis and facilitating regenerative growth within the ductal compartment. Further studies are needed to examine the factors that direct this regenerative process toward the acinar compartment.

Abbreviations

MG, meibomian gland; MGP, meibomian gland probing; o-MGD, obstructive meibomian gland dysfunction; OARREBS, orifice-associated rete ridge epithelial/basement membrane structures; RR, rete ridge; DWECL, duct wall epithelial cell layers; DWT, duct wall thickness; IVCM, in vivo confocal microscopy; PDF, periductal fibrosis.

Data Sharing Statement

All data relevant to the study are included in the article.

Ethics Approval and Informed Consent

This research, involving the collection and study of existing data and documents, was recorded by the investigator in such a manner that subjects could not be identified directly or through identifiers linked to them. This study received an institutional review board exempt review determination by WCG IRB, an independent institutional review board.

Author Contributions

SLM and CT planned and conducted the study, analyzed the data, as well as drafted and revised manuscript. CT performed statistical analysis. SLM is guarantor. All authors made a significant contribution to the work reported, whether that is in the conception, study design, execution, acquisition of data, analysis and interpretation, or in all these areas; took part in drafting, revising or critically reviewing the article; gave final approval of the version to be published; have agreed on the journal to which the article has been submitted; and agree to be accountable for all aspects of the work.

Funding

This study did not receive any specific grants from any funding agency in the public, commercial or not-for-profit sectors.

Disclosure

SLM is the owner (>5% stock holder) of MGD Innovations, Inc., which holds patents on instrumentation and methods for intraductal diagnosis and treatment of meibomian gland disease (MGD), and related patents on the use of jojoba-based treatment options for MGD. The authors report no other conflicts of interest in this work.

References

1. Bron AJ, de Paiva CS, Chauhan SK, et al. Tfos dews ii pathophysiology report. *Ocular Surf*. 2017;15(3):438–510. doi:10.1016/j.jtos.2017.05.011
2. Tomlinson A, Bron AJ, Korb DR, et al. The international workshop on meibomian gland dysfunction: report of the diagnosis subcommittee. *Invest Ophthalmol Vis Sci*. 2011;52(4):2006–2049. doi:10.1167/iovs.10-6997f
3. Knop E, Knop N, Millar T, Obata H, Sullivan DA. The International Workshop on Meibomian Gland Dysfunction: report of the Subcommittee on Anatomy, Physiology, and Pathophysiology of the Meibomian gland. *Invest Ophthalmol Visual Sci*. 2011;52(4):1938–1978. doi:10.1167/iovs.10-6997c
4. Xie H-T, Sullivan DA, Chen D, Hatton MP, Kam WR, Liu Y. Biomarkers for progenitor and differentiated epithelial cells in the human meibomian gland. *Stem Cells Transl Med*. 2018;7(12):887–892. doi:10.1002/sctm.18-0037
5. Parfitt GJ, Geyfman M, Xie Y, Jester JV. Characterization of quiescent epithelial cells in mouse meibomian glands and hair follicle/sebaceous glands by immunofluorescence tomography. *J invest dermatol*. 2015;135(4):1175. doi:10.1038/jid.2014.484
6. Lavker R, Treet J, Sun T. Label-retaining cells (LRCs) are preferentially located in the ductal epithelium of the meibomian gland: implications on the mucocutaneous junctional (MCJ) epithelium of the eyelid. *Invest Ophthalmol Visual Sci*. 2003;44(13):3781.
7. Reneker LW, Yang X, Zhong X, Huang AJW. Meibomian gland (MG) acinar regeneration from atrophy in a Fgfr2 conditional knockout mouse model. *Invest Ophthalmol Visual Sci*. 2019;60(9):1412.
8. Yang X, Reneker LW, Zhong X, Huang AJ, Jester JV. Meibomian gland stem/progenitor cells: the hunt for gland renewal. *Ocular Surf*. 2023;29:497–507. doi:10.1016/j.jtos.2023.07.004
9. Tchegnon E, Liao C-P, Ghotbi E, et al. Epithelial stem cell homeostasis in Meibomian gland development, dysfunction, and dry eye disease. *JCI Insight*. 2021;6(20). doi:10.1172/jci.insight.151078
10. Maskin SL. Rete ridge structures form meibomian gland distal external duct wall and basal epithelial layer. *Invest Ophthalmol Visual Sci*. 2022;63(7):1967–A0297.
11. Zhou S, Robertson DM. Wide-field in vivo confocal microscopy of meibomian gland acini and rete ridges in the eyelid margin. *Invest Ophthalmol Visual Sci*. 2018;59(10):4249–4257. doi:10.1167/iovs.18-24497
12. Shen Z, Sun L, Liu Z, et al. Rete ridges: morphogenesis, function, regulation, and reconstruction. *Acta Biomater*. 2022;155:19–34.

13. Maskin SL, Alluri S. Expressible meibomian glands have occult fixed obstructions: findings from meibomian gland probing to restore intraductal integrity. *Cornea*. 2019;38(7):880–887. doi:10.1097/ICO.0000000000001954
14. Parfitt GJ, Lewis PN, Young RD, et al. Renewal of the holocrine meibomian glands by label-retaining, unipotent epithelial progenitors. *Stem Cell Rep*. 2016;7(3):399–410. doi:10.1016/j.stemcr.2016.07.010
15. Maskin SL, Testa WR. Growth of meibomian gland tissue after intraductal meibomian gland probing in patients with obstructive meibomian gland dysfunction. *Br J Ophthalmol*. 2018;102(1):59–68. doi:10.1136/bjophthalmol-2016-310097
16. Maskin SL, Alluri S. Intraductal meibomian gland probing: background, patient selection, procedure, and perspectives. *Clin Ophthalmol*. 2019;13:1203–1223. doi:10.2147/OPTH.S183174
17. Maskin SL, Alluri S. Meibography guided intraductal meibomian gland probing using real-time infrared video feed. *Br J Ophthalmol*. 2020;104 (12):1676. doi:10.1136/bjophthalmol-2019-315384
18. Kheirkhah A, Kobashi H, Girgis J, Jamali A, Ciolino JB, Hamrah P. A randomized, sham-controlled trial of intraductal meibomian gland probing with or without topical antibiotic/steroid for obstructive meibomian gland dysfunction. *Ocular Surf*. 2020;18(4):852–856. doi:10.1016/j.jtos.2020.08.008
19. Huang X, Qin Q, Wang L, Zheng J, Lin L, Jin X. Clinical results of Intraductal Meibomian gland probing combined with intense pulsed light in treating patients with refractory obstructive Meibomian gland dysfunction: a randomized controlled trial. *BMC Ophthalmol*. 2019;19(1):211. doi:10.1186/s12886-019-1219-6
20. Incekalan TK, Harbiyeli II, Yagmur M, Erdem E. Effectiveness of intraductal meibomian gland probing in addition to the conventional treatment in patients with obstructive meibomian gland dysfunction. *Ocul Immunol Inflammation*. 2018;26(1):1–7. doi:10.1080/09273948.2018.1426300
21. Ma X, Lu Y. Efficacy of intraductal meibomian gland probing on tear function in patients with obstructive meibomian gland dysfunction. *Cornea*. 2016;35(6):725–730. doi:10.1097/ICO.0000000000000777
22. Dongju Q, Hui L, Jianjiang X. Clinical research on intraductal meibomian gland probing in the treatment of patients with meibomian gland dysfunction. *Chin J Optom Ophthalmol*. 2014;16(10):615–621.
23. Warren NA, Maskin SL. Review of literature on intraductal meibomian gland probing with insights from the inventor and developer: fundamental concepts and misconceptions. *Clin Ophthalmol*. 2023;17:497–514. doi:10.2147/OPTH.S390085
24. Maskin SL, Warren NA. *Your Dry Eye Mystery Solved: Reversing Meibomian Gland Dysfunction, Restoring Hope*. Yale University Press; 2022.
25. Yamaguchi M, Kutsuna M, Uno T, Zheng X, Kodama T, Ohashi Y. Marx line: fluorescein staining line on the inner lid as indicator of meibomian gland function. *Am J Ophthalmol*. 2006;141(4):669–669. e668. doi:10.1016/j.ajo.2005.11.004
26. Karakus S, Dai X, Zhu X, Gottsch JD. The role of lid margin structures in the meibomian gland function and ocular surface health. *Expert Rev Ophthalmol*. 2021;16(1):11–18. doi:10.1080/17469899.2021.1826309
27. Ha M, Kim JS, Hong S-Y, et al. Relationship between eyelid margin irregularity and meibomian gland dropout. *Ocular Surf*. 2021;19:31–37. doi:10.1016/j.jtos.2020.11.007
28. Lee HK, Lee KS, Kim JK, Kim HC, Seo KR, Kim EK. Epithelial healing and clinical outcomes in excimer laser photorefractive surgery following three epithelial removal techniques: mechanical, alcohol, and excimer laser. *Am J Ophthalmol*. 2005;139(1):56–63. doi:10.1016/j.ajo.2004.08.049
29. Wijnholds J. "Basal cell migration" in regeneration of the corneal wound-bed. *Stem Cell Rep*. 2019;12(1):3–5. doi:10.1016/j.stemcr.2018.12.009
30. Itty S, Hamilton SS, Baratz KH, Diehl NN, Maguire LJ. Outcomes of epithelial debridement for anterior basement membrane dystrophy. *Am J Ophthalmol*. 2007;144(2):217–221. e212. doi:10.1016/j.ajo.2007.04.024
31. Hamada S, Darrad K, McDonnell PJ. Salzmann's nodular corneal degeneration (SNCD): clinical findings, risk factors, prognosis and the role of previous contact lens wear. *Contact Lens Anterior Eye*. 2011;34(4):173–178. doi:10.1016/j.clae.2011.02.004
32. Yoon JJ, Ismail S, Sherwin T. Limbal stem cells: central concepts of corneal epithelial homeostasis. *World J Stem Cells*. 2014;6(4):391. doi:10.4252/wjsc.v6.i4.391
33. Jimenez-Rojo L, Granchi Z, Graf D, Mitsiadis TA. Stem cell fate determination during development and regeneration of ectodermal organs. *Front Physiol*. 2012;3:107. doi:10.3389/fphys.2012.00107
34. Maskin SL. Intraductal meibomian gland probing relieves symptoms of obstructive meibomian gland dysfunction. *Cornea*. 2010;29(10):8. doi:10.1097/ICO.0b013e3181d836f3
35. Nakayama N, Kawashima M, Kaido M, Arita R, Tsubota K. Analysis of meibum before and after intraductal meibomian gland probing in eyes with obstructive meibomian gland dysfunction. *Cornea*. 2015;34(10):1206–1208. doi:10.1097/ICO.0000000000000558
36. Srinivasan B, Eakins K. The reepithelialization of rabbit cornea following single and multiple denudation. *Exp Eye Res*. 1979;29(6):595–600. doi:10.1016/0014-4835(79)90014-9
37. Giannaccare G, Taroni L, Senni C, Scorcia V. Intense pulsed light therapy in the treatment of meibomian gland dysfunction: current perspectives. *Clin Optom*. 2019;11:113–126. doi:10.2147/OPTO.S217639